Original Article

MOLECULAR METABOLISM

Deletion of *Ascl1* in pancreatic β-cells improves insulin secretion, promotes parasympathetic innervation, and attenuates dedifferentiation during metabolic stress

Anna B. Osipovich [1,2], Frank Y. Zhou [3], Judy J. Chong [3], Linh T. Trinh [4], Mathew A. Cottam [2], Shristi Shrestha [2], Jean-Philippe Cartailler [2], Mark A. Magnuson [1,2,4,*]

ABSTRACT

Objective: ASCL1, a pioneer transcription factor, is essential for neural cell differentiation and function. Previous studies have shown that *Ascl1* expression is increased in pancreatic β-cells lacking functional K_{ATP} channels or after feeding of a high fat diet (HFD) suggesting that it may contribute to the metabolic stress response of β-cells.

Methods: We generated β-cell-specific *Ascl1* knockout mice ($Ascl1^{\beta KO}$) and assessed their glucose homeostasis, islet morphology and gene expression after feeding either a normal diet or HFD for 12 weeks, or in combination with a genetic disruption of *Abcc8*, an essential K_{ATP} channel component.

Results: *Ascl1* expression is increased in response to both a HFD and membrane depolarization and requires CREB-dependent Ca^{2+} signaling. No differences in glucose homeostasis or islet morphology were observed in $Ascl1^{\beta KO}$ mice fed a normal diet or in the absence of K_{ATP} channels. However, male $Ascl1^{\beta KO}$ mice fed a HFD exhibited decreased blood glucose levels, improved glucose tolerance, and increased β-cell proliferation. Bulk RNA-seq analysis of islets from $Ascl1^{\beta KO}$ mice from three studied conditions showed alterations in genes associated with the secretory function. HFD-fed $Ascl1^{\beta KO}$ mice showed the most extensive changes with increased expression of genes necessary for glucose sensing, insulin secretion and β-cell proliferation, and a decrease in genes associated with β-cell dysfunction, inflammation and dedifferentiation. HFD-fed $Ascl1^{\beta KO}$ mice also displayed increased expression of parasympathetic neural markers and cholinergic receptors that was accompanied by increased insulin secretion in response to acetylcholine and an increase in islet innervation.

Conclusions: A*scl1* expression is induced by stimuli that cause Ca^{2+}-signaling to the nucleus and contributes in a multifactorial manner to the loss of β-cell function by promoting the expression of genes associated with cellular dedifferentiation, attenuating β-cells proliferation, suppressing acetylcholine sensitivity, and repressing parasympathetic innervation of islets. Thus, the removal of *Ascl1* from β-cells improves their function in response to metabolic stress.

Keywords Ascl1; Pancreatic beta cell; Metabolic stress; Dedifferentiation; Insulin secretion; Islet innervation

1. INTRODUCTION

Type 2 diabetes (T2D) is a multi-system disorder that is characterized by insulin resistance, hyperglycemia, nutrient overload and metabolic stress-induced loss of pancreatic β-cell mass and/or function [1—4]. Cellular dedifferentiation and the loss of β-cell identity are important contributors to β-cell dysfunction in the setting of insulin resistance and metabolic stress [5,6]. Dedifferentiation is characterized by the loss of key β-cell genes that control essential cellular processes, such as glucose sensing and insulin secretion, and the upregulation of genes associated with immature pancreatic endocrine cell states. The signaling pathways and transcriptional regulators that drive these changes in metabolically stressed β-cells are not understood [7,8].

ASCL1 (Achaete-scute homolog 1), also known as MASH1, is a basic helix-loop-helix (bHLH) transcription factor involved in neuronal fate determination [9]. Like other bHLH proteins, ASCL1 must either homodimerize or form heterodimers with other bHLH proteins to bind to the hexanucleotide binding motif CANNTG, also known as an E-box [10]. During development, the dynamic expression of *Ascl1* promotes both the proliferation and differentiation of neural stem cells [11] with ASCL1 being both necessary and sufficient to induce the formation of functional neurons from non-neuronal cells [12]. *Ascl1* is also critical

[1]Department of Molecular Physiology and Biophysics, Vanderbilt University, Nashville, TN 37232, USA [2]Center for Stem Cell Biology, Vanderbilt University, Nashville, TN 37232, USA [3]College of Arts and Sciences, Vanderbilt University, Nashville, TN 37232, USA [4]Department of Cell and Developmental Biology, Vanderbilt University, Nashville, TN 37232, USA

*Corresponding author. 9465 MRB-IV, 2213 Garland Avenue, Nashville, TN 37232-0494, USA. Fax: +1 615 322 6645. E-mail: mark.magnuson@vanderbilt.edu (M.A. Magnuson).

Received August 2, 2023 • Revision received September 20, 2023 • Accepted September 22, 2023 • Available online 26 September 2023

https://doi.org/10.1016/j.molmet.2023.101811

for development of neuroendocrine cells in multiple tissues, including stomach, lung, adrenal medulla, thyroid and prostate [13–15]. Since ASCL1 targets both readily accessible and closed regions of chromatin in developing neural cells, it is considered a pioneer transcription factor [16,17].

We previously reported that *Ascl1* expression is increased in two different models of metabolically stressed β-cells: HFD-fed mice and mice lacking the K_{ATP} channel subunit *Abcc8* [18,19]. In *Abcc8* knockout (KO) β-cells, a sustained increase in intracellular Ca^{2+} ($[Ca^{2+}]_i$), or excitotoxicity, resulting from chronic membrane depolarization leads to impairments in islet morphology, glucose tolerance, and β-cell identity [19,20]. We have shown that expression of *Ascl1* in β-cells is increased following treatments that cause Ca^{2+} influx, and have performed detailed transcriptomic analyses that have suggested that ASCL1 is an upstream regulator for many of the genes upregulated in *Abcc8* KO islets, including for *Aldh1a3*, a marker of β-cell dedifferentiation [19]. *Ascl1* has also been shown to be expressed at higher levels in less mature β-cells that exhibit increased $[Ca^{2+}]_i$ [21]. While *Ascl1b* regulates pancreatic endocrine cell fate in zebrafish [22], *Ascl1* is not required for pancreatic endocrine cell specification or the expression of pro-endocrine transcription factor *Neurog3* during mouse development [23]. *ASCL1* is expressed in human islets, its gene exhibits an open chromatin structure in β-cells [24], and islet-specific super-enhancers are located nearby [25]. Since super-enhancers are often located near key cell identity genes [26], these observations further suggest that *ASCL1* may be important for regulating the function of β-cells in a yet-to-be-defined manner. Altogether, these data led us to hypothesize that the induction of *Ascl1* in response to metabolic stress contributes to β-cell failure in T2D by regulating the gene network that is induced in β-cells in response to metabolic stress and promoting β-cell dedifferentiation.

To determine the role of *Ascl1* in metabolic-stress induced β-cell failure, we generated pancreatic β-cell-specific *Ascl1* knockout mice and assessed β-cell function and gene expression in response to 1) a normal diet, 2) metabolic stress brought on by a HFD, and 3) excitotoxic stress caused by a genetic ablation of *Abcc8*. Our results indicate that ASCL1 contributes to the loss of β-cell identity and function in the setting of HFD-induced metabolic stress. Mice with a β-cell-specific ablation of *Ascl1* exhibit improved glucose tolerance, increased β-cell proliferation, increased expression of β-cell identity genes and decreased expression of dedifferentiation markers. In addition, islets of HFD-fed that lack *Ascl1* exhibit increased islet innervation and increased insulin secretion in response to acetylcholine.

2. MATERIALS AND METHODS

2.1. Mouse lines and husbandry

The *Ascl1*^{Flox} (*Ascl1*^{tm2Fgu}) [27], *Ins*^{Cre} (*Ins1*$^{tm1.1(cre)Thor}$) [28], *Gt(ROSA)26*$^{Sortm9(CAG-tdTomato)Hze}$ [29] and *Abcc8* KO (*Abcc8*$^{tm1.1Mgn}$) [20] alleles were all maintained as C57Bl/6J congenic lines (stock 000664 at The Jackson Laboratory). At weaning (3–4 weeks of age), mice were fed normal chow (NC) (4.5% fat content, PicoLab, 5L0D) or a HFD (60% fat content, D12492, Research Diets) for 12 weeks. All animal experimentation was performed under the oversight of the Vanderbilt Institutional Animal Care and Use Committee. Mice were genotyped by PCR using primers listed in Table S1.

2.2. Glucose homeostasis

Blood glucose concentrations were determined in tail blood samples using a BD Logic glucometer. Intraperitoneal glucose tolerance tests (IPGTT) were performed following a 16-hour overnight fast. Blood glucose concentrations were measured at 0, 15, 30, 60, and 120 min after administering D-glucose (2 mg/g body mass). Plasma insulin concentrations were measured by radioimmunoassay (Millipore, PI-13K) and performed in triplicate by the Vanderbilt Hormone Assay and Analytical Services Core.

2.3. Islet isolation and culture

Islets were isolated by the Vanderbilt Islet and Pancreas Analysis (IPA) core by injecting 0.6 mg/mL collagenase P (Roche) into the pancreatic bile duct followed by a Histopaque-1077 (Sigma) fractionation and hand-picking. Isolated islets were cultured were cultured overnight in low glucose DMEM (Thermo, 11966-025) containing 1 g/L glucose and supplemented with 10% FBS (Atlanta Biologicals), 4.6 mM HEPES, 1% penicillin/streptomycin (Thermo), 1% non-essential amino acids (Sigma) in a sterile cell incubator at 37 °C with 5% CO_2 infusion and 95% humidity. Islet responses were assessed by treatments with culture media containing high glucose (20 mM), 100 μM tolbutamide (Sigma, T0891), 50 μM verapamil (Sigma, V4629) or 1 μM for CREB-inhibitor 666-15 (MedChemExpress, HY-101120). Control samples were treated only with the DMSO vehicle (0.1%). To measure static glucose-stimulated insulin secretion, islets from HFD-fed male mice were cultured overnight then equilibrated in KRHB (Krebs-Ringer HEPES Buffer, pH7.4) for 30 min followed by 30 min incubation with KRHB containing either low glucose (3.3 mM), high glucose (16.7 mM), high glucose with 100 nM Extendin-4 (MedChemExpress, HY-13443) or 1 μM acetylcholine (MedChemExpress, HY-B0282). Insulin concentrations in post-incubation supernatants were measured by radioimmunoassay.

2.4. RNA isolation and RT-qPCR

RNA was isolated from whole islets using the Maxwell 16 LEV simplyRNA Tissue Kit (Promega, TM351). For qPCR, reverse transcription was performed using a High Capacity cDNA Reverse Transcription Kit (Thermo). 2 ng of cDNA was used to perform real-time qPCR using Power SYBR Green PCR master mix (Thermo) and a CFX96 Real-Time PCR system (Bio-Rad). Relative expression was determined by the ΔCt method by normalizing to the expression of *Actb*. Primers are listed in Table S1.

2.5. RNA sequencing and data analysis

RNA quality was assessed using an Agilent 2100 Bioanalyzer and only those samples with an RNA integrity number (RIN) 7 or above were used to produce cDNA libraries using a Low Input Library Prep Kit. 150 nucleotide paired-end reads were obtained by Novogene Corp. using an Illumina NovaSeq6000 instrument that resulted in at least 40 M raw sequencing reads per sample. The Spliced Transcripts Alignment to a Reference (STAR v2.6.0c) application [30] was used to perform sequence alignments to the mm10 (GRCm38) mouse genome reference and GENCODE comprehensive gene annotations (Release M17). Overall, 85–87% of the raw sequencing reads were uniquely mapped to genomic sites. DESeq2 was employed for additional sample-level quality control analysis and downstream pairwise comparisons [31]. Gene ontology analysis of differentially expressed genes was performed using Metascape [32]. LISA analysis was used to predict transcriptional regulators of differentially expressed genes [33].

For analysis of *ASCL1* expression in human β-cells, scRNA-seq data for human normal and T2D islets were obtained from the human pancreas atlas program (HPAP) [34] and downloaded in the anndata.h5ad format. Raw counts were normalized and Log + 1 transformed using Scanpy v1.9.3 [35]. To explore *ASCL1* and *INS* expression, cells were filtered for β-cells based on annotations provided by HPAP.

ASCL1^{+} β-cells were defined as cells with greater than 0 normalized counts for *ASCL1*. β-Cells were binned into three discretized bins using the pandas qcut function with q = 3 and using expression of *INS* as the input. Cells with fewer than 8.343 log normalized counts for *INS* were defined as low, those with greater than 8.631 log normalized counts as high, and those in between as moderate.

2.6. Immunohistochemistry and morphometric analysis

Whole pancreata were fixed for 2 h in 4% paraformaldehyde, incubated overnight at 4 °C in 30% sucrose, embedded in OCT compound (Tissue Tek), frozen on dry ice, and sectioned at a depth of 10 mm. Immunostaining was performed as previously described [36]. Primary antibodies used were guinea pig anti-insulin (Linco, 1:1000), rabbit anti-glucagon (Linco, 1:1000), rabbit anti-somatostatin (Linco 1:1000), guinea pig anti-pancreatic polypeptide (Linco, 1:1000), goat anti-dsRed (Santa Cruz Biotechnology, 1:1000), rabbit anti-ALDH1A3 (Novus Biologicals,1:500), and mouse anti-TUJ (BioLegend, 1:2000). Secondary antibodies were donkey anti-guinea pig and anti-mouse IgG Alexa-488 conjugated, donkey anti-goat IgG Alexa-555 conjugated and donkey anti-rabbit IgG Alexa-647 conjugated (Thermo, 1:1000). After antibody staining, slides were mounted with Invitrogen Prolong Gold Antifade Mountant with DAPI (Thermo). Images were acquired using an Aperio ScanScope CS imaging system or Zeiss LSM Meta 510 confocal microscope. Quantifications of relative areas were done on evenly spaced pancreatic sections at 150 μm apart by using ImageJ software [37]. Insulin^{+} β-cell areas were calculated as a percentage of the whole pancreas areas (DAPI^{+}), relative hormone+ areas, and relative TUJ+ areas as a percentage of total islet areas and β-cell proliferation as a percentage of MKI+ cell per insulin+ cells. Images in figures are representative of the phenotype observed in at least three different animals per genotype.

2.7. Statistical analysis

p-Values were determined by ANOVA or by a two-tailed unpaired Student's t-test where applicable.

3. RESULTS

3.1. *Ascl1* expression is elevated in dedifferentiated and metabolically stressed β-cells and requires Ca^{2+} signaling through CREB

To better understand the developmental expression pattern of *Ascl1* during pancreas and pancreatic β-cell development, we began by extracting a temporal expression profile for *Ascl1* from our prior transcriptional network analysis of FACS-purified cell populations [38]. As shown in Figure 1A, *Ascl1* is expressed during the pre-pancreatic and multipotent endocrine progenitor cell stages (embryonic days (E) 9.5—10.5) and is then down-regulated beginning at E15.5 in normal pre-endocrine and β-cell lineages. The highest levels of *Ascl1* expression were observed in two less differentiated progenitor cell states caused either by the genetic deletion of *Neurog3* or *Insm1* [38]. While *Ascl1* is expressed at very low levels in normal adult β-cells, we have previously shown that it is induced 2- and 30-fold, respectively, by metabolic stress due to overnutrition (5 weeks on a HFD) or by excitotoxicity due to the lack of functional K_{ATP} channels (*Abcc8* KO) (Figure 1B) [18]. In this study, islets isolated from HFD-fed (12 weeks) and *Abcc8* KO mice had similarly increased levels of *Ascl1* (Figure 1C). 24-hour *in vitro* incubations of wild type (WT) islets with the K_{ATP} channel inhibitor tolbutamide, which causes membrane depolarization, leads to increased *Ascl1* expression that is diminished with the addition either of the voltage-dependent Ca^{2+} channel (VDCC) inhibitor verapamil or CREB inhibitor 666-15 (Figure 1D). CREB (cAMP Response Element-Binding protein) is an important Ca^{2+}-signaling activated regulator of transcription [39], and analysis of available CREB ChIP data shows that promoters for human and mouse *Ascl1* contain nearby CREB-bound regions (Figure S1). Analysis of scRNA-seq data from human islets of control and T2D individuals [34] showed that higher *ASCL1* expression occurs in β-cells that have lower expression of *INS* in T2D (Figure 1E, F). Combined, these data indicate that *Ascl1* expression is increased in metabolically stressed β-cells, that less differentiated endocrine cells exhibit higher expression than mature β-cells, and that the induction of *Ascl1* in adult β-cells occurs in response to treatments that cause an increase $[Ca^{2+}]_i$ and requires CREB-dependent Ca^{2+}-signaling to the nucleus.

3.2. Glucose homeostasis and islet morphology are unaffected in adult *Ascl1*$^{\beta KO}$ mice fed a normal diet (ND)

To determine the role of *Ascl1* in β-cells, we crossed *Ascl1*^{Flox} and *Ins1*^{Cre} mice to obtain animals that lack *Ascl1* specifically in β-cells (*Ascl1*$^{\beta KO}$). In addition, to assess the efficiency of Cre-recombination and to lineage trace β-cells we also introduced a Cre-activated red fluorescent protein (RFP) reporter *Rosa26*^{tdTomato} allele in the breeding scheme (Figure 2A). Analysis of the number of RFP^{+} cells per Ins^{+} cells showed that we achieved more than 95% efficiency of Cre recombination in β-cells (Figure 2B) and observed an expected decrease in *Ascl1* in islets by RT-qPCR (Figure 2C). Next, to assess the impact of *Ascl1* on normal β-cell development and function we analyzed glucose homeostasis and islet morphology of adult 14 weeks old mice fed a ND. Male *Ascl1*$^{\beta KO}$ animals, wild type (WT) controls, and mice heterozygous for the *Ascl1*^{Flox} allele (Het) all had similar weight, blood glucose and insulin levels, glucose tolerance and insulin responses (Figure 3A—G) with female mice also showing no differences (Figure S2). Immunofluorescent staining of pancreatic sections and quantification showed no difference in the percentage of β-cell area per total pancreatic area, INS^{+} to RFP^{+} area ratio (a measure of maintenance of β-cell identity), or the percentage of hormone^{+} area (insulin, glucagon, somatostatin and pancreatic polypeptide) per islet area (Figure 3H—K). Islet architecture also appeared normal (Figure 3J). Since *Ascl1*$^{\beta KO}$ mice survive into adulthood and demonstrate no significant differences in glucose homeostasis and islet composition we conclude that *Ascl1* does not measurably affect β-cell development or function in a metabolically unstressed state.

3.3. *Ascl1*$^{\beta KO}$ mice have decreased blood glucose, improved glucose tolerance and increased β-cell proliferation after 12 weeks on a HFD

To investigate the role of *Ascl1* in β-cell response to metabolic stress due to nutrient overload we fed *Ascl1*$^{\beta KO}$ and control mice a HFD for 12 weeks prior to accessing glucose homeostasis and the β-cell area and proliferation. While male animals gained similar amounts of weight, *Ascl1*$^{\beta KO}$ males exhibited a decrease in their fed blood glucose levels, an increase in glucose tolerance, and a trend towards higher plasma insulin levels (Figure 4A—G). At the same time, immunostaining and quantification revealed a trend in the increased total β-cell area ($p = 0.09$), no changes in the INS^{+} to RFP^{+} area ratio and a significant increase in the number of proliferating MKI67^{+} β-cells in *Ascl1*$^{\beta KO}$ male mice (Figure 4H—K). We did not observe any significant changes in glucose homeostasis in HFD-fed female mice (Figure S3). The combination of decreased blood glucose levels, improved glucose tolerance, and increased β-cell proliferation in the absence of *Ascl1* in male animals fed a HFD indicates that metabolic stress-induced expression of *Ascl1* impairs both β-cell function and proliferation.

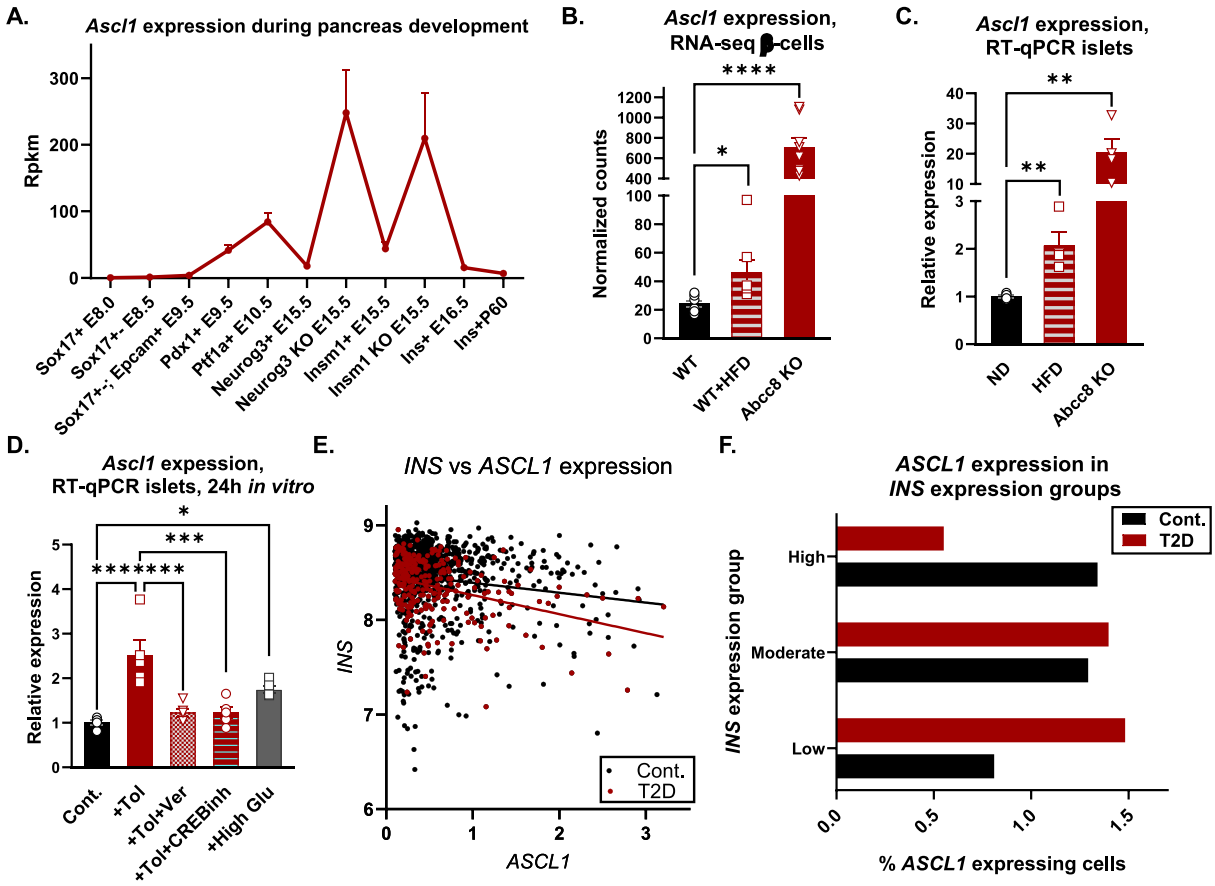

Figure 1: Increases in $[Ca^{2+}]_i$ and CREB-dependent Ca^{2+} signaling increase *Ascl1* expression in β-cells. A) Expression levels of *Ascl1* mRNA profiled by RNA-seq in sorted pancreatic developmental lineages: gut tube endoderm (Sox17$^+$ at E8.0/8.5), posterior foregut endoderm (*Pdx1*$^+$ at E9.5), pancreatic multipotent progenitor cells (*Ptf1a*$^+$ at E10.5), endocrine progenitor cells (*Neurog3*$^+$ and *Insm1*$^+$ at E15.5), nascent β-cells (Ins$^+$ at E16.5), and adult β-cells (Ins$^+$ at P60). Two profiled mutant conditions for endocrine progenitor cells (*Neurog3*$^{-/-}$ and *Insm1*$^{-/-}$ at E15.5) indicate that *Ascl1* is increased in the absence of *Neurog3* and *Insm1*. N = 3. **B)** RNA-seq of purified β-cells shows that *Ascl1* expression is increased in wild type (WT) mice on HFD (WT + HFD, 5 weeks) and in *Abcc8* KO mice. N = 8 (males and females, 8 weeks old). **C)** RT-qPCR analysis of isolated islets shows the increase in *Ascl1* expression on HFD and in *Abcc8* KO mice in comparison to ND mice. N = 4 (males, 14–17 weeks old). **D)** RT-qPCR analysis of islets from *in vitro* incubations of WT islets shows that tolbutamide or high glucose (Glu, 20 mM) lead to an increase in *Ascl1* expression that is decreased with the addition of verapamil and CREB inhibitor (N = 4, males, 8 weeks old). Error bars: ±SEM. **p ≤ 0.01; *p ≤ 0.05. p-value determined by ANOVA. **(E, F)** Analysis of scRNA-seq data of human β-cells from the human pancreas atlas program (HPAP). **E)** Scatter plot of insulin (*INS*) versus *ASCL1* expression in *ASCL1*-expressing human β-cells from normal (935 cells) and T2D (280 cells) individuals shows that higher *ASCL1* expression is associated with lower insulin expression in T2D. **F)** *ASCL1*-expressing human β-cells were divided into three groups based on levels of *INS* expression. The bar graph shows that the percentage of *ASCL1*-expressing cells per group is higher in low-insulin expressing cells in T2D.

3.4. *Ascl1*$^{\beta KO}$ mice do not show an improvement in glucose homeostasis or islet architecture on a global *Abcc8* KO background

Since *Ascl1* expression is strongly up-regulated in a genetic model of excitotoxicity (*Abcc8* knockout (KO) mice) we next sought to determine whether the loss of *Ascl1* affects β-cell function on a global *Abcc8* KO background. Adult *Abcc8* KO mice develop glucose intolerance after 12 weeks of age and have a disrupted islet architecture and compromised β-cell identity [18,19]. After interbreeding, we obtained *Ascl1*$^{\beta KO}$; *Abcc8* KO mice as well as *Abcc8* KO controls which were assessed at 14 weeks of age on a ND for alterations in glucose homeostasis and islet composition. Surprisingly, we did not observe any improvements in blood glucose levels, glucose tolerance or insulin secretion in this cohort of mice (Figure 5A–H, Figure S4). We also did not observe any changes in the β-cell area, the INS$^+$ to RFP$^+$ area ratio, or islet composition. Islets retained the disrupted architecture characteristic of *Abcc8* KO mice with α- and δ-cells being found intermingling with β-cells within the core of the islets (Figure 5H–K). These results indicate that disruption of *Ascl1* is not sufficient by itself to rescue the β-cell dysfunction of *Abcc8* KO mice.

3.5. Transcriptional profiling of *Ascl1*$^{\beta KO}$ islets in three different conditions reveals variable changes in secretory and neural genes

To determine how the absence of *Ascl1* in β-cells affects different cellular responses, we next performed bulk RNA-seq of islets from male *Ascl1*$^{\beta KO}$ and Het littermate control male mice from the ND, HFD and *Abcc8* KO cohorts (n = 4 for each condition, 14–17 weeks old). Principal component analysis of each transcriptome revealed a clear separation between three different conditions with the HFD condition demonstrating the largest difference between *Ascl1*$^{\beta KO}$ and control islets (Figure 6A). Differential expression (DE) analysis revealed 605, 1685 and 589 genes whose expression was altered (FDR $p_{adj} < 0.05$) in ND, HFD and *Abcc8* KO conditions, respectively (Table S2), with the most profound ASCL1-dependent transcriptional changes occurring in the HFD-fed islets, consistent with our phenotyping results. Overlap analysis of the genes affected by the absence of *Ascl1* in the three different conditions showed only small similarities, indicating that each of the different treatment conditions caused a distinct response (Figure 6B). Notably, among the genes that were commonly dysregulated in all conditions three are required for neural exocytosis: *Syt1*,

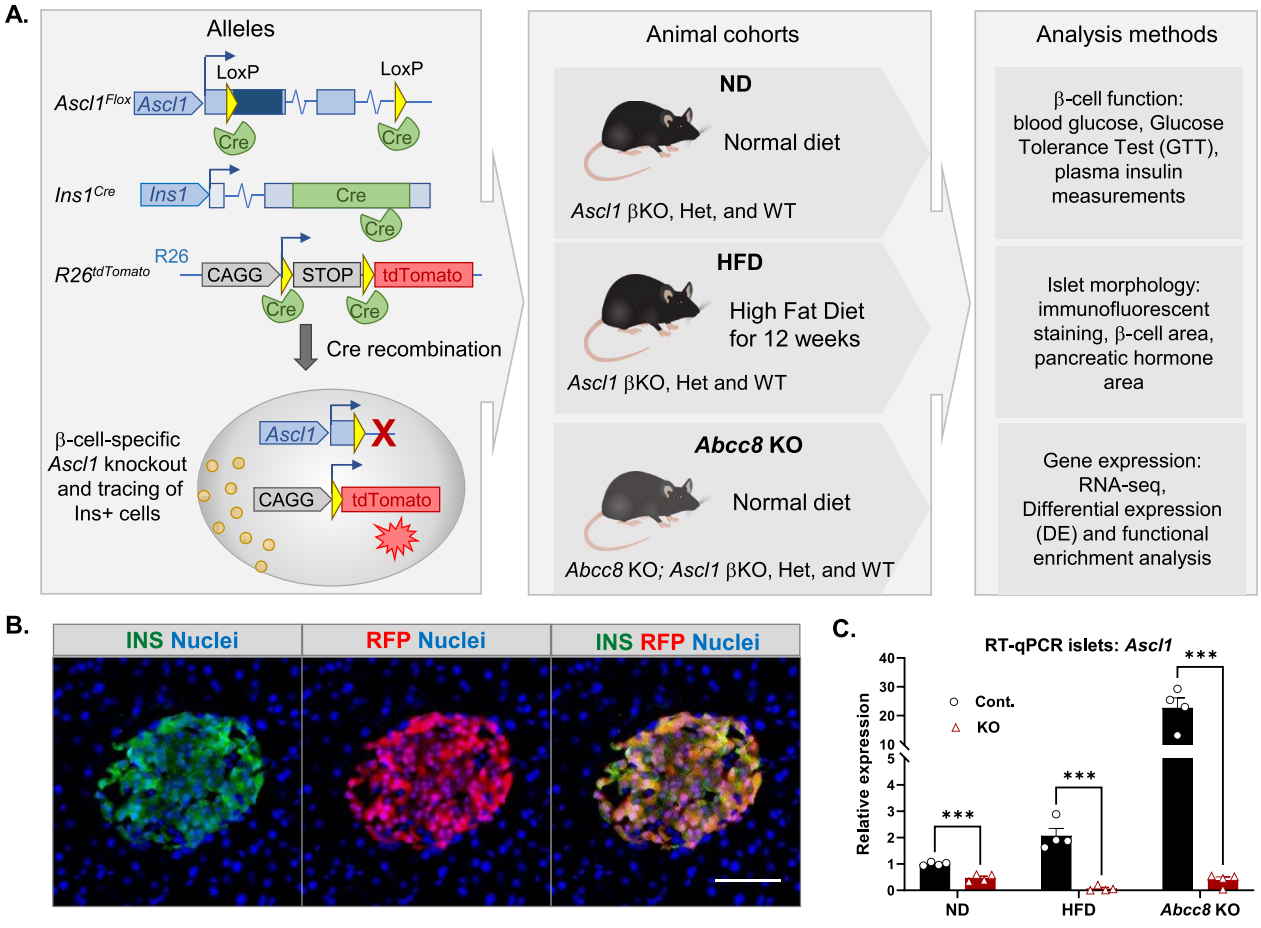

Figure 2: Generation and analysis of β-cell specific *Ascl1* knockout mice (*Ascl1*$^{\beta KO}$). A) Summary of alleles that were bred together to create *Ascl1*$^{\beta KO}$ and control heterozygous (Het) and wild type (WT) mice, animal cohorts that were used in the study including normal diet (ND), high fat diet (HFD) and *Abcc8* homozygous KO groups, and analyses that were performed. **B)** Immunofluorescent co-staining of *Ascl1* Het islets with anti-insulin and anti-RFP antibodies demonstrates high efficiency Cre-recombination in β-cells. Scale bar: 50 μM. C) RT-qPCR analysis of islets of *Ascl1*$^{\beta KO}$ mice in ND, HFD and *Abcc8* KO conditions shows a significant decrease in *Ascl1* expression in comparison to Het controls. N = 4 (males 14–17 weeks old). Error bars: ±SEM. ***p ≤ 0.001. p-value determined by t-test.

Pak6, and *Dclk1*. Despite the small number of shared genes, comparative gene ontology (GO)-based functional enrichment analysis of the datasets from the different conditions indicated that ASCL1-dependent genes shared several functional categories (Figure 6C, Table S3). The shared GO categories include protein localization, cell secretion and export from cell, synaptic signaling, neural system development, cell junction and adhesion, and ER-to-Golgi vesicle traffic (Figure 6D), indicating that ASCL1 regulates genes involved with the secretory function of islets.

To predict the transcriptional co-regulators that might act in concert with ASCL1 we used the epigenetic *Landscape In Silico deletion Analysis* (LISA) tool. This analysis method has been used to identify upstream transcription factors and chromatin regulators that mediate the perturbation of specific DE gene sets [33]. Our use of LISA revealed a diverse and only partially overlapping set of positive and negative drivers of upregulated and downregulated DE genes, respectively (Figure 6E, Table S3). Notably, ASCL1 was identified as the upstream driver of genes that are upregulated in the absence of *Ascl1* in all three conditions, implying that ASCL1 functions as a repressor of gene expression in β-cells. Conversely, in the HFD condition, ASCL1 was identified as one of the top drivers of down-regulated genes, implying that it activates gene expression in this setting. These findings suggest that transcriptional regulation by ASCL1 in β-cells is complex and dependent on both the treatment condition and genotype. The observed complexity is consistent with ASCL1 action being dependent on other co-regulators, including other bHLH neuronal transcription factors, thereby differentially regulating many neural and secretory genes in response to the ND, HFD and *Abcc8* KO conditions.

3.6. β-Cell identity and metabolic stress genes affected by HFD are oppositely regulated in *Ascl1*$^{\beta KO}$ islets

While ASCL1 regulates a wide spectrum of neural and secretory genes, nearly three times more genes were affected in the HFD compared to the ND and *Abcc8* KO conditions. Although we did not detect any significant alterations in β-cell function in the ND fed *Ascl1*$^{\beta KO}$ islets, transcriptional profiling revealed 309 up-regulated and 296 down-regulated genes. Functional enrichment analysis indicates that the upregulated genes are involved in cell morphogenesis, neuronal projection, and ECM organization, whereas the down-regulated genes are involved in ER protein transport and cell cycle regulation (Figure S5, Tables S2 and S3). Similarly, even though *Ascl1* is highly expressed in *Abcc8* KO β-cells, its deletion affected only 268 up-regulated and 321 down-regulated genes in the *Ascl1*$^{\beta KO}$; *Abcc8* KO islets. This relatively low number is in marked contrast to the 7393 dysregulated

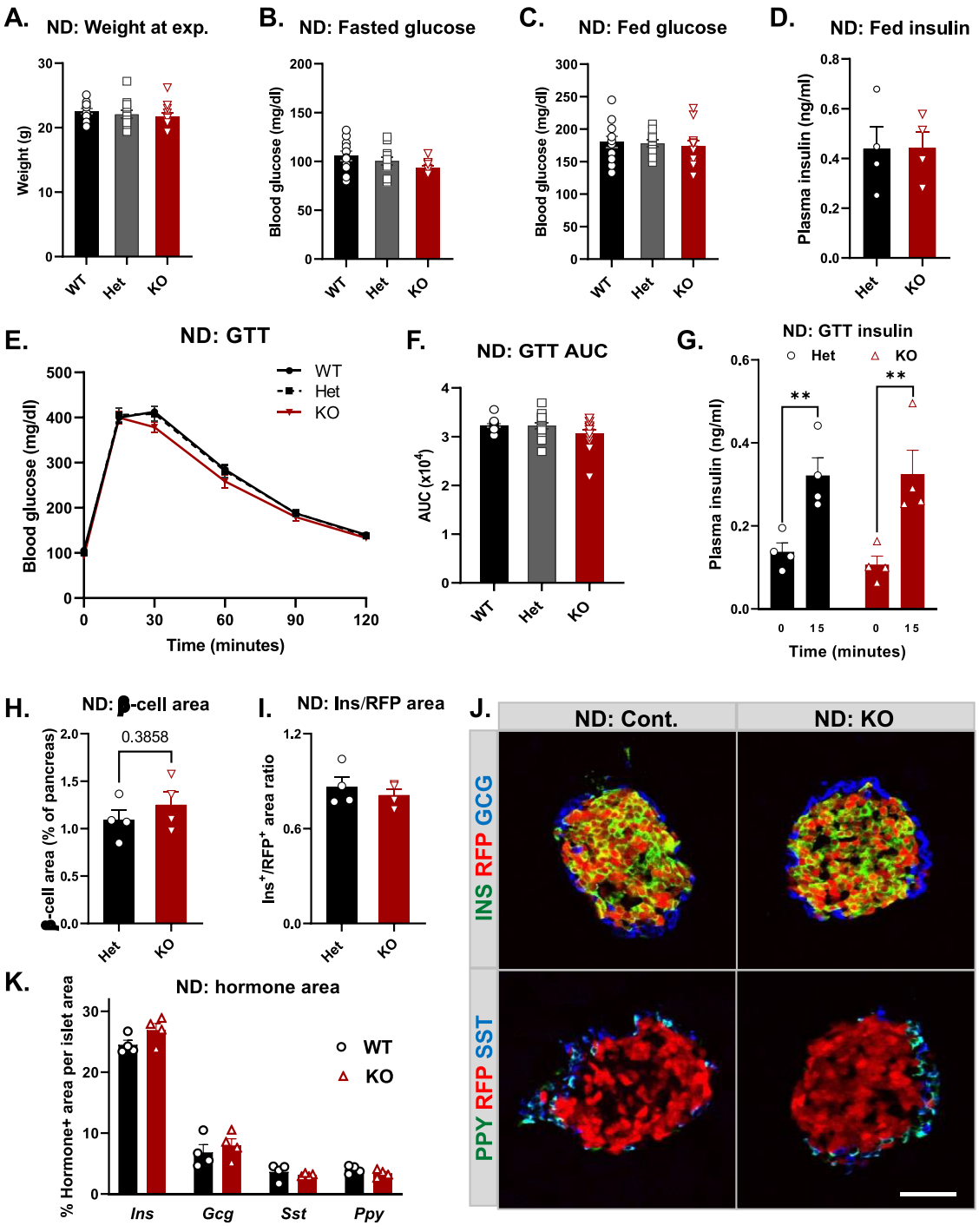

Figure 3: Glucose homeostasis and islet composition are unaffected in adult *Ascl1*$^{\beta KO}$ mice fed a normal diet (ND). A) Body weight measurements at the time of the experiment and fasted **(B)** and fed **(C)** blood glucose concentration measurements showed no significant differences between *Ascl1*$^{\beta KO}$ (KO) and control Het and WT animals. N = 12. **D)** Random-fed plasma insulin levels. N = 4. **E)** Intraperitoneal glucose tolerance test (GTT) and area under the curve (AUC) measurements for **(F)**. N = 12. **G)** Insulin secretion in response to glucose injection in GTT for *Ascl1*$^{\beta KO}$ and control Het samples. Both genotypes show an equal increase in plasma insulin concentration 15 min after glucose injection. N = 4. **H**–**K)** Immunofluorescent staining and quantification of pancreatic islet tissues from *Ascl1*$^{\beta KO}$ (KO) and control (cont.) Het mice. **H)** Quantification of β-cell (INS^{+}) area as the percentage of total pancreas area. N = 4. **I)** Quantification of INS+ to RFP+ area ratio in islets as a measurement of β-cell dedifferentiation. N = 4. **J)** Representative images of immunofluorescent staining for red fluorescent protein (RFP, red) and pancreatic hormones insulin (INS, green), glucagon (GCG, blue), somatostatin (SST, blue) and pancreatic polypeptide (PPY, green) of *Ascl1*$^{\beta KO}$ and control Het samples. Scale bar: 50 μM. **K)** Quantification of hormone-positive areas per total islet areas. N = 4. All mice are males, 14 weeks old. Error bars: ±SEM. *p ≤ 0.05. p-value was determined by ANOVA or by t-test were applicable. (For interpretation of the references to color in this figure legend, the reader is referred to the Web version of this article.)

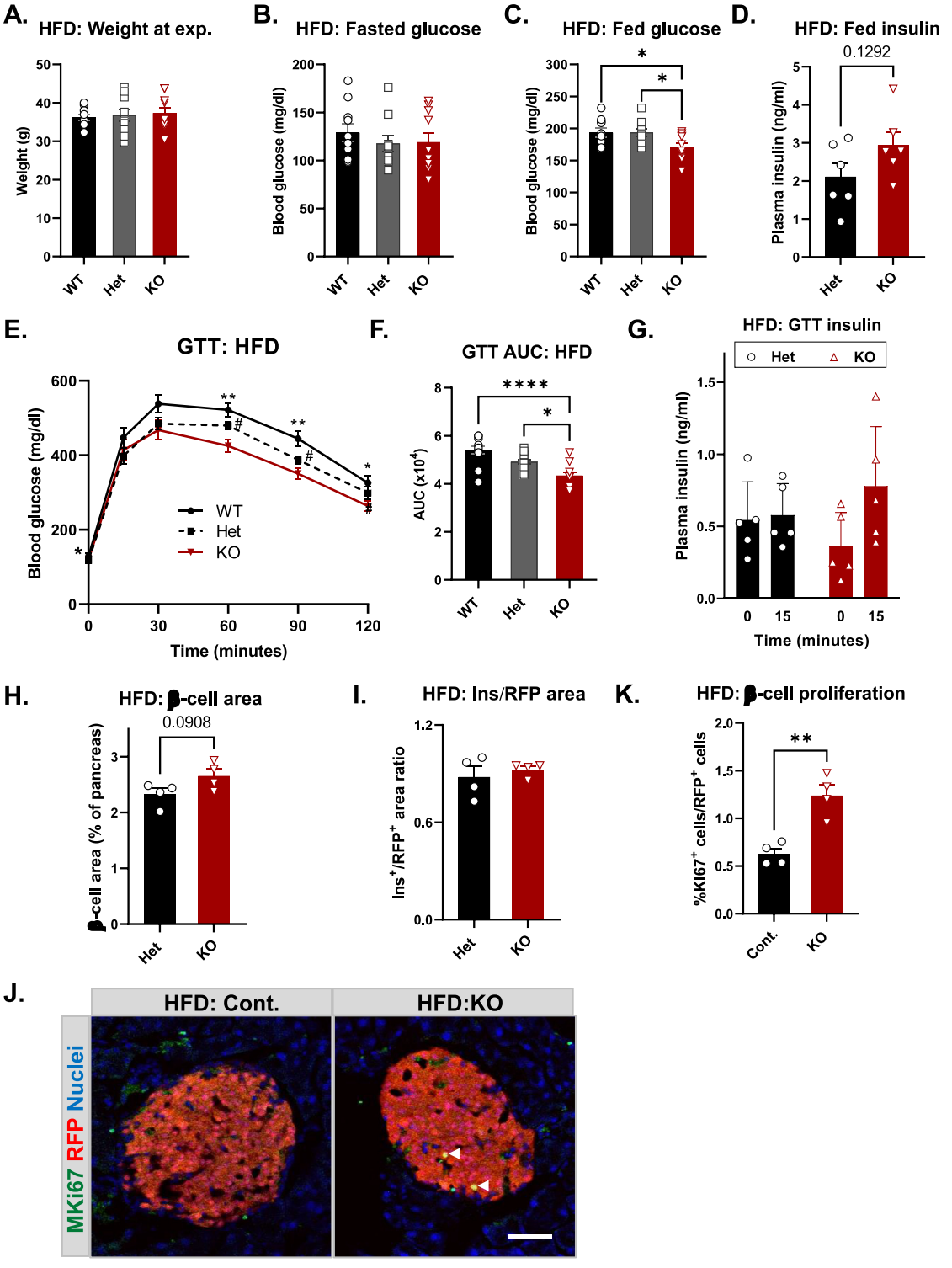

Figure 4: *Ascl1*$^{\beta KO}$ mice have decreased blood glucose, improved glucose tolerance and increased β-cell proliferation after 12 weeks on a high fat diet (HFD). A) Body weight measurements at the time of the experiment and fasted **(B)** and fed **(C)** blood glucose concentration measurements between *Ascl1*$^{\beta KO}$ (KO) and control Het and WT animals on HFD. *Ascl1*$^{\beta KO}$ mice have decreased fed blood glucose concentration. N = 10. **D)** Random-fed plasma insulin levels for *Ascl1*$^{\beta KO}$ and control Het samples. N = 6. **E)** Intraperitoneal glucose tolerance test (GTT) and its area under the curve (AUC) measurements **(F)** show that *Ascl1*$^{\beta KO}$ mice have improved glucose tolerance on HFD. N = 10. **G)** Insulin secretion in response to glucose injection in GTT for *Ascl1*$^{\beta KO}$ and control Het samples on HFD. N = 5. **H–K)** Immunofluorescent staining and quantification of pancreatic islet tissues from *Ascl1*$^{\beta KO}$ (KO) and control (cont.) Het mice on HFD. **H)** Quantification of β-cell (INS^{+}) area as the percentage of total pancreas area. N = 4. **I)** Quantification of INS+ to RFP+ area ratio in islets as a measurement of β-cell dedifferentiation. N = 4. **J)** Representative images of immunofluorescent staining for red fluorescent protein (RFP, red) that marks β-cells and cell proliferation marker MKI67 (green) of *Ascl1*$^{\beta KO}$ and control (cont.) Het samples. Nuclei are stained with DAPI (blue). Arrows show MKI67-positive β-cells. Scale bar: 50 μM. **K)** Quantification of β-cell proliferation. N = 4. All mice are males, 17 weeks old. Error bars: ±SEM. ******p ≤ 0.0001, **p ≤ 0.01, *p ≤ 0.05. p-value was determined by ANOVA or by t-test were applicable. (For interpretation of the references to color in this figure legend, the reader is referred to the Web version of this article.)

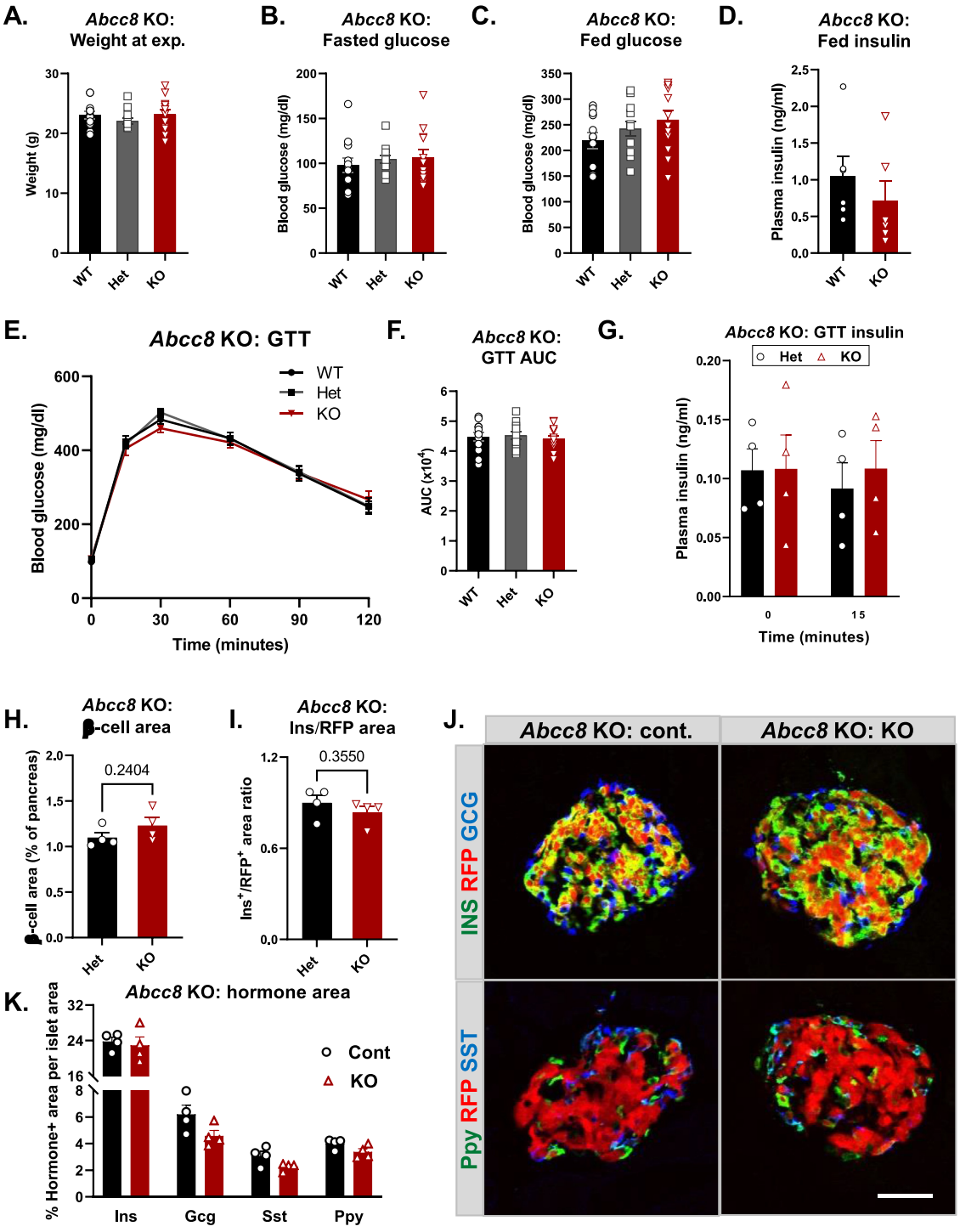

Figure 5: ***Ascl1*$^{\beta KO}$ mice do not show an improvement in glucose homeostasis or an islet architecture on a global *Abcc8* KO background. A)** Body weight measurements at the experiment and fasted **(B)** and fed **(C)** blood glucose concentration measurements showed no significant differences between *Ascl1*$^{\beta KO}$ (KO) and control Het and WT animals on *Abcc8* KO background. N = 12. **D)** Random-fed plasma insulin levels. N = 6. **E)** Intraperitoneal glucose tolerance test (GTT) and its area under the curve (AUC) measurements for **(F)**. N = 12. **G)** Insulin secretion in response to glucose injection in GTT. Both genotypes show defects in the increase in plasma insulin concentration 15 min after glucose injection. N = 4. **H–K)** Immunofluorescent staining and quantification of pancreatic islet tissues from *Ascl1*$^{\beta KO}$ (KO) and control (cont.) Het mice on *Abcc8* KO background. **H)** Quantification of β-cell (INS^{+}) area as the percentage of total pancreas area. N = 4. **I)** Quantification of the INS+ to RFP+ area ratio in islets as a measurement of β-cell dedifferentiation. N = 4. **J)** Representative images of immunofluorescent staining for red fluorescent protein (RFP) and pancreatic hormones insulin (INS), glucagon (GCG), somatostatin (SST) and pancreatic polypeptide (PPY) of *Ascl1*$^{\beta KO}$ and control Het samples. Nuclei are stained with DAPI (blue). Scale bar: 50 μM. **K)** Quantification of hormone-positive areas per total islet areas. N = 4. All mice are males, 14 weeks old. Error bars: ±SEM. p-value was determined by ANOVA or by t-test were applicable. (For interpretation of the references to color in this figure legend, the reader is referred to the Web version of this article.)

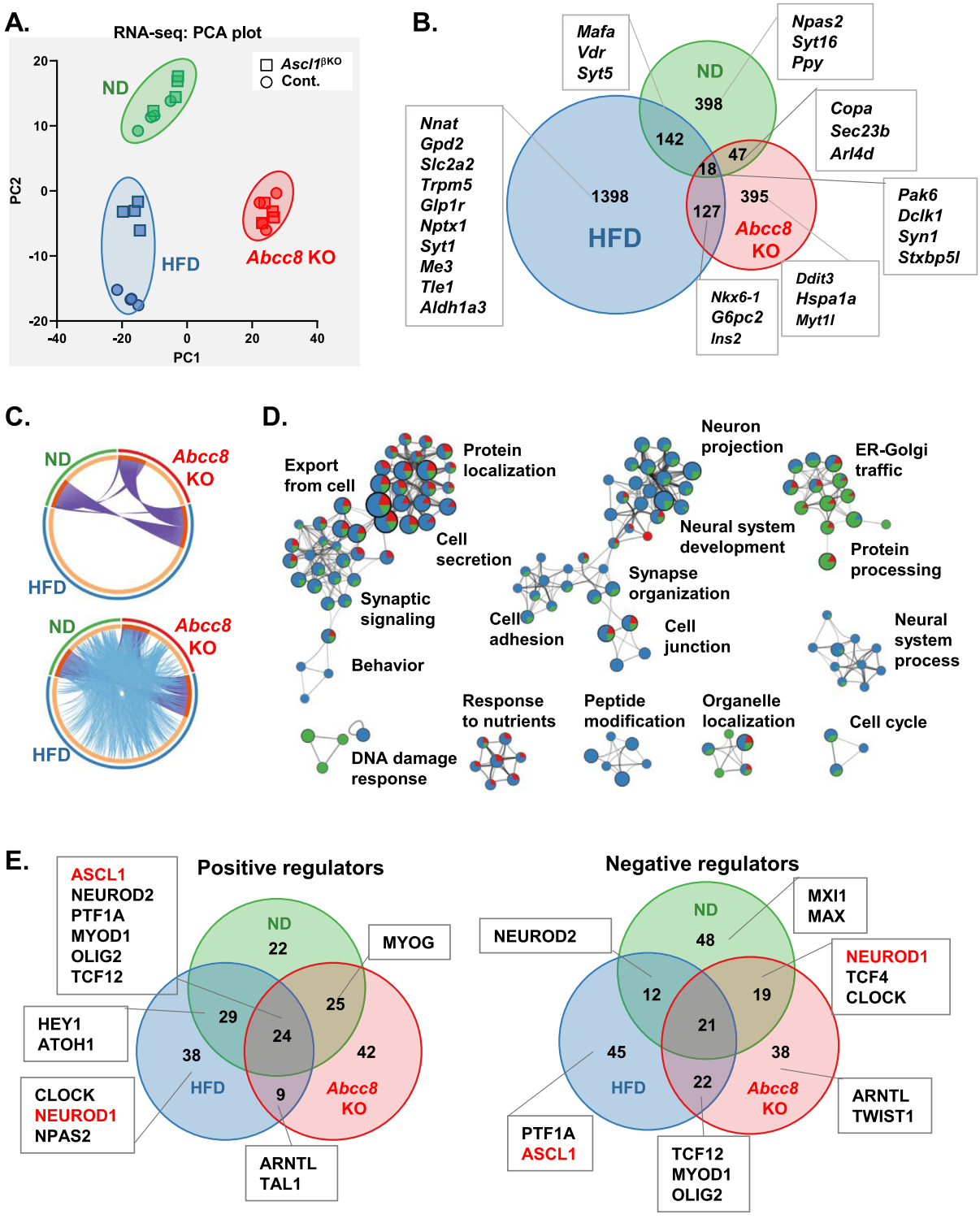

Figure 6: RNA-seq of *Ascl1*$^{\beta KO}$ islets in three different conditions reveals variable changes in secretory and neural genes. A) PCA plot of RNA-seq samples. ND, normal diet (light green, *Ascl1*$^{\beta KO}$ ND vs control (cont.) ND comparison), HFD, high fat diet (light blue, *Ascl1* $^{\beta KO}$ HFD vs cont. HFD comparison), *Abcc8* KO (pink, *Ascl1* $^{\beta KO}$ *Abcc8* KO vs control *Abcc8* KO comparison). Male mice, 14–17 weeks old. **B)** Venn diagram indicating overlap between differentially expressed (DE) genes ($p_{adj} < 0.05$) identified from pairwise comparisons for each condition, with select dysregulated genes indicated for each overlap. ND, normal diet (light green, *Ascl1* KO ND vs cont. ND comparison), HFD, high fat diet (light blue, *Ascl1* KO HFD vs cont. HFD comparison), *Abcc8* KO (pink, *Ascl1* KO *Abcc8* KO vs cont. *Abcc8* KO comparison). **C)** Cord diagrams show genes (purple curves) and GO terms/pathways (blue curves) shared among lists of DE genes from three comparisons. ND, green; HFD, blue; *Abcc8* KO, red. **D)** Enrichment network visualization of enriched functional GO terms/pathways shared among DE genes from the three comparisons. Node size is proportional to the number of genes in the GO category, with pie charts indicating a proportion of genes from each comparison: ND, green; HFD, blue; *Abcc8* KO, red. Intensity of a node border color indicates the GO category enrichment p-value (from 10^{-48} to 10^{-2}). **E)** Venn diagrams indicating overlap between the top 100 transcriptional regulators predicted to drive the expression of upregulated DE genes (positive regulators) and downregulated genes (negative regulators) for each of the three comparisons. bHLH transcription factors are shown in callouts for each overlap. ND, light green; HFD, light blue; *Abcc8* KO, pink. ASCL1 is among the predicted regulators. (For interpretation of the references to color in this figure legend, the reader is referred to the Web version of this article.)

genes in FACS-purified *Abcc8* KO β-cells [18], suggesting that ASCL1 is only partially responsible for the many gene expression changes brought on by the lack of functional K_{ATP} channels. Interestingly, the top genes upregulated in *Ascl1*$^{\beta KO}$ islets on *Abcc8* KO background are involved in ER stress response (*Hspa1a/b*, *Ddit3*, *Ddit4*), autophagy (*Depp1*, *Gabarapl1*) and chromatin maintenance (*H3c6*, *H4c12*) and down-regulated genes involved in hormone secretion and vesicle transport (*Chgb*, *G6pc2, Kdelr*) (Figure S6, Tables S2 and S3). The increases in stress genes and decreases in secretory genes in the absence of *Ascl1* indicate that it may play a limited protective role in β-cells in the absence of *Abcc8*, however its deletion does not result in any significant functional changes in *Abcc8* KO β-cells.

The transcriptional effects of the *Ascl1* deletion were more pronounced in HFD-fed mice where 923 genes were up-regulated and 757 down-regulated (Figure 7A). To compare *Ascl1*-driven changes on HFD to transcriptional alterations in normal islets caused by HFD feeding, we also compared the control ND and control HFD samples. The results show that metabolic stress caused by HFD feeding leads to major

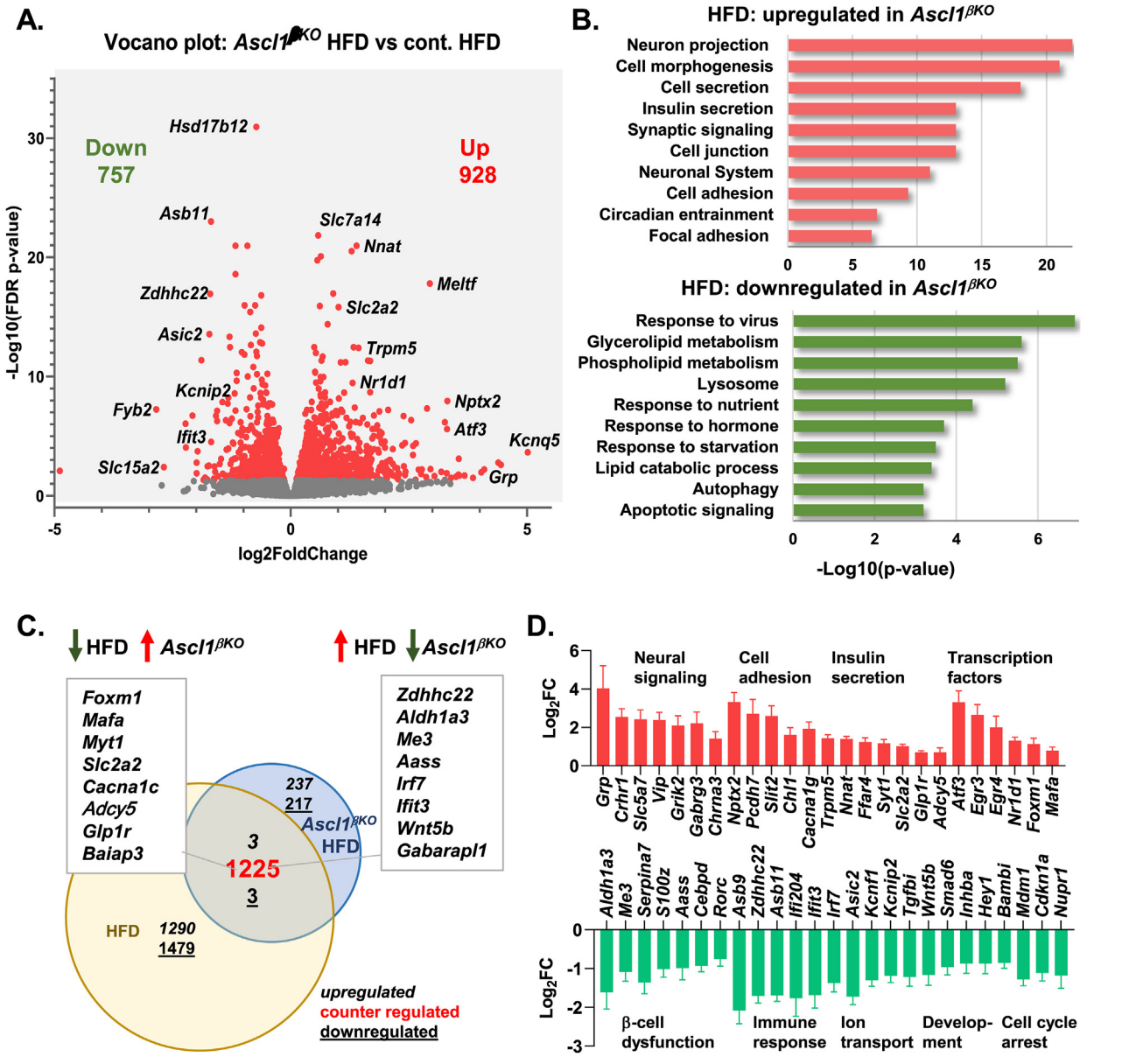

Figure 7: β-cell identity and metabolic stress genes affected by HFD are oppositely regulated in *Ascl1*$^{\beta KO}$ islets. A) Volcano plot (Log_2 FoldChange (FC) over FDR p_{adj}-value) showing differentially expressed (DE) genes with red dots ($p_{adj} < 0.05$) in *Ascl1* $^{\beta KO}$ HFD vs control (cont.) comparison. HFD islets from 17-week-old male mice (N = 4). Select top differentially expressed genes (based on p_{adj}-value) are indicated by names and total numbers of downregulated (green) and upregulated (red) genes are provided. **B)** Functional enrichment analysis of upregulated and downregulated DE genes in *Ascl1* $^{\beta KO}$ HFD vs control HFD islet comparison. Select top enriched pathways are shown. **C)** Venn diagram indicating directional overlaps between DE genes identified from pairwise comparisons for effects of HFD (Control HFD vs control ND) and for effects of *Ascl1* on HFD (*Ascl1* $^{\beta KO}$ HFD vs control HFD). A large proportion of genes (shown in red) that are affected by HFD are changed in a opposite direction when *Ascl1* is deleted. Select oppositely regulated genes are shown in callouts. **D)** Differential expression of select top upregulated and downregulated DE genes in *Ascl1* $^{\beta KO}$ HFD vs control HFD islets comparison that are also oppositely regulated in control HFD vs control ND comparison. Text indicates gene functional associations. Log_2FC: Log_2 Fold Change. (For interpretation of the references to color in this figure legend, the reader is referred to the Web version of this article.)

changes in islet transcriptome with 4003 dysregulated genes (2173 up- and 1830 down-regulated) (Figure S7A, Table S2). The GO categories of up-regulated genes included lipid metabolism, autophagy, ER stress and immune response whereas those for down-regulated genes included cell morphogenesis, neuron projection, cell secretion, synapse organization and cell adhesion (Figure S7B,C). All of these changes are consistent with the now well-established view that metabolically stressed β-cells undergo ER stress, inflammation, and a progressive loss of cell identity. However, and in marked contrast, in HFD-fed islets that lack *Ascl1* many of these adverse changes are reversed. Functional enrichment analysis indicated that upregulated genes are involved in cell morphogenesis, neuron projection, cell secretion, synaptic signaling, cell junction and adhesion, and down-regulated genes are involved in immune response to virus, lipid metabolism, lysosome, autophagy and apoptotic signaling (Figure 7B, Table S3), a response profile that is nearly opposite to that of the HFD islets. Indeed, the directional overlap analysis of islet genes dysregulated by a HFD showed that most of the 1225 genes that are either up- or down-regulated in response to the HFD are oppositely regulated in the absence of *Ascl1* (Figure 7C). Notably, the genes down-regulated by the HFD but up-regulated in the *Ascl1*$^{\beta KO}$ on HFD include many involved in neural signaling (*Grp*, *Crhr1*, *Vip*), neurotransmitter receptors (*Grik2*, *Gabrg3*, *Chrna3*), cell junction and adhesion molecules (*Nptx2*, *Pcdh7*, *Slit2*, *Chl1*) and many genes that are involved in positive regulation of insulin secretion (*Trpm5*, *Nnat*, *Ffar4*, *Syt1*, *Slc2a2*, *Glp1r*, *Adcy5, Baiap3*). Additionally, key β-cell transcription factors (*Mafa*, *Mafb*, *Myt1*, *Nkx6-1*, *Neurod1*), early stress response genes (*Atf3*, *Egr3, Egr4*), and essential β-cell proliferation genes (*Foxm1*, *Mki67*) are also up-regulated. Conversely, genes normally up-regulated on HFD but down-regulated in the absence of *Ascl1* include well established markers for β-cell dedifferentiation (*Aldh1a3, Aass, Serpin7a*) [40], immune response (*Irf7*, *Ifit3*), β-cell dysfunction and hyperglycemia (*S100z*) [41], developmental genes (*Wnt5b*, *Bambi*), genes involved in protein palmitoylation (*Zdhhc22*) and ubiquitination (*Asb9*, *Asb11*), and negative regulators of the cell cycle (*Nupr1*, *Cdkn1a*) (Figure 7C,D). Combined, these data indicate that transcriptional regulation by ASCL1 and, potentially, other co-regulators that are simultaneously induced by metabolic stress contribute substantially to the loss of β-cell function through the activation of dedifferentiation program and repression of a network of β-cell identity genes involved in insulin secretion and proliferation.

3.7. Decreased dedifferentiation and increased insulin secretion and islet innervation in *Ascl1*$^{\beta KO}$ islets on HFD

To validate the beneficial transcriptional changes that the deletion of *Ascl1* has on islets from HFD-fed mice, we performed qPCR for selected genes and confirmed that genes critical for insulin secretion (*Atf3*, *Trpm5*, *Chrna3*, *Foxm1*, *Slc2a2*, *Glp1r*, *Nptx2*) are up-regulated in the *Ascl1*$^{\beta KO}$ islets and genes indicating β-cell dysfunction (*Aldh1a3*, *Serpina7*, *Asb11*, *Nupr1*, *Me3*, *S100z*, *Cdkn1a*) are down-regulated (Figure 8A, B). Immunofluorescent staining of islet sections of HFD-fed mice also confirmed the decrease in levels of the β-cell dedifferentiation marker ALDH1A3 in *Ascl1*$^{\beta KO}$ islets compared to controls (Figure 8C). Together, these results further confirm that deletion of *Ascl1* from β-cells diminish the HFD-induced expression of dedifferentiation markers, including ALDH1A3.

Finally, given the increase in pro-secretory genes, including *Chrna3*, a receptor for the parasympathetic neurotransmitter acetylcholine, we measured glucose-stimulated insulin secretion in static islet incubations of *Ascl1*$^{\beta KO}$ and control islets from HFD-fed mice. Both genotypes showed significant increases in insulin secretion in response to high glucose, high glucose and extendin-4, a GLP1 receptor agonist, and acetylcholine, compared to low glucose alone (Figure 8D). While the *Ascl1*$^{\beta KO}$ samples exhibited a trend towards more insulin secretion in response to of all tested secretagogues, the combination of high glucose and acetylcholine resulted in the most robust and significant increase (Figure 8D). Given the enhanced response to acetylcholine, increased expression of neuropeptides *Vip* and *Grp*, and the elevated amounts of *Slc18a3* and *n-NOS (Nos1)*, two well established markers of parasympathetic nerves, we next sought to determine whether *Ascl1*$^{\beta KO}$ islets might have increased density of cholinergic nerve fibers. Immunostaining for TUJ (TUBB3), a neuron-specific form of tubulin, and measurement of TUJ^{+} area per islet area revealed an increase in the number of neuronal processes that both penetrate and surround pancreatic islets, indicating that neural innervation in the *Ascl1*$^{\beta KO}$ islets from HFD-fed mice is increased (Figure 8E,F). These findings indicate that *Ascl1*$^{\beta KO}$ islets secrete more insulin in response to acetylcholine and exhibit increased parasympathetic innervation.

4. DISCUSSION

In this study we assessed the role of *Ascl1* in mediating the metabolic stress response of pancreatic β-cells. Our findings indicate that ASCL1 contributes to a loss of β-cell function both by activating a dedifferentiation program and by suppressing the expression of secretory and innervation genes in response to HFD feeding. Due to these effects, deletion of *Ascl1* improves β-cell function during metabolic stress brought on by overnutrition.

4.1. Ca^{2+} signaling induces *Ascl1* expression

In β-cells, Ca^{2+} signaling is critical for glucose-stimulated insulin secretion [42] but prolonged increases in $[Ca^{2+}]_i$ due to chronic metabolic stress may cause β-cell dysfunction [43,44]. It was previously shown [4,45] that there is a rise in $[Ca^{2+}]_i$ in β-cells in HFD-fed mice and *db/db* mice. *Abcc8* KO mice have a sustained increase in $[Ca^{2+}]_i$, increased Ca^{2}-signaling to the nucleus, and marked alterations in the β-cell transcriptome that impair cell function [18,19]. In neurons and cardiomyocytes, two other excitable cell types, excess Ca^{2+}-signaling, or excitotoxicity [46], is an established cause of cellular dysfunction [47–49]. While β-cells have functional and transcriptional similarities with neurons [50], and transcriptional regulation by ASCL1 has a well-established role in neural cell differentiation and function, the involvement of *Ascl1* in physiological responses of β-cells has not been previously explored.

Here we show that during pancreatic β- and endocrine cell development *Ascl1* is expressed in multipotent pancreatic progenitor cells and is strongly increased in the absence of *Neurog3* or *Insm1*, two TFs necessary for the functional endocrine cell differentiation [51,52]. While *Ascl1* is not essential for formation of islets in mice [23], our findings indicate that *Ascl1* is most highly expressed in mis-differentiated or dedifferentiated pancreatic endocrine progenitor cells. Conversely, in adult mouse β-cells in normal condition *Ascl1* is expressed at very low levels. Thus, while *Ascl1* does not appear to play any significant role in determining endocrine cell fates, it acts as a response factor that is induced in response to elevations of $[Ca^{2+}]_i$, such as those brought on in animals either by HFD feeding or the deletion of *Abcc8*, or in isolated islets by short-term stimulation with high glucose or tolbutamide treatment. Our observations that treatment of isolated islets with verapamil and a CREB inhibitor abrogate tolbutamide-induced expression of *Ascl1*, and the prior identification of multiple CREB-binding sites near the *Ascl1* promoter (Figure S1), are all consistent with *Ascl1* gene

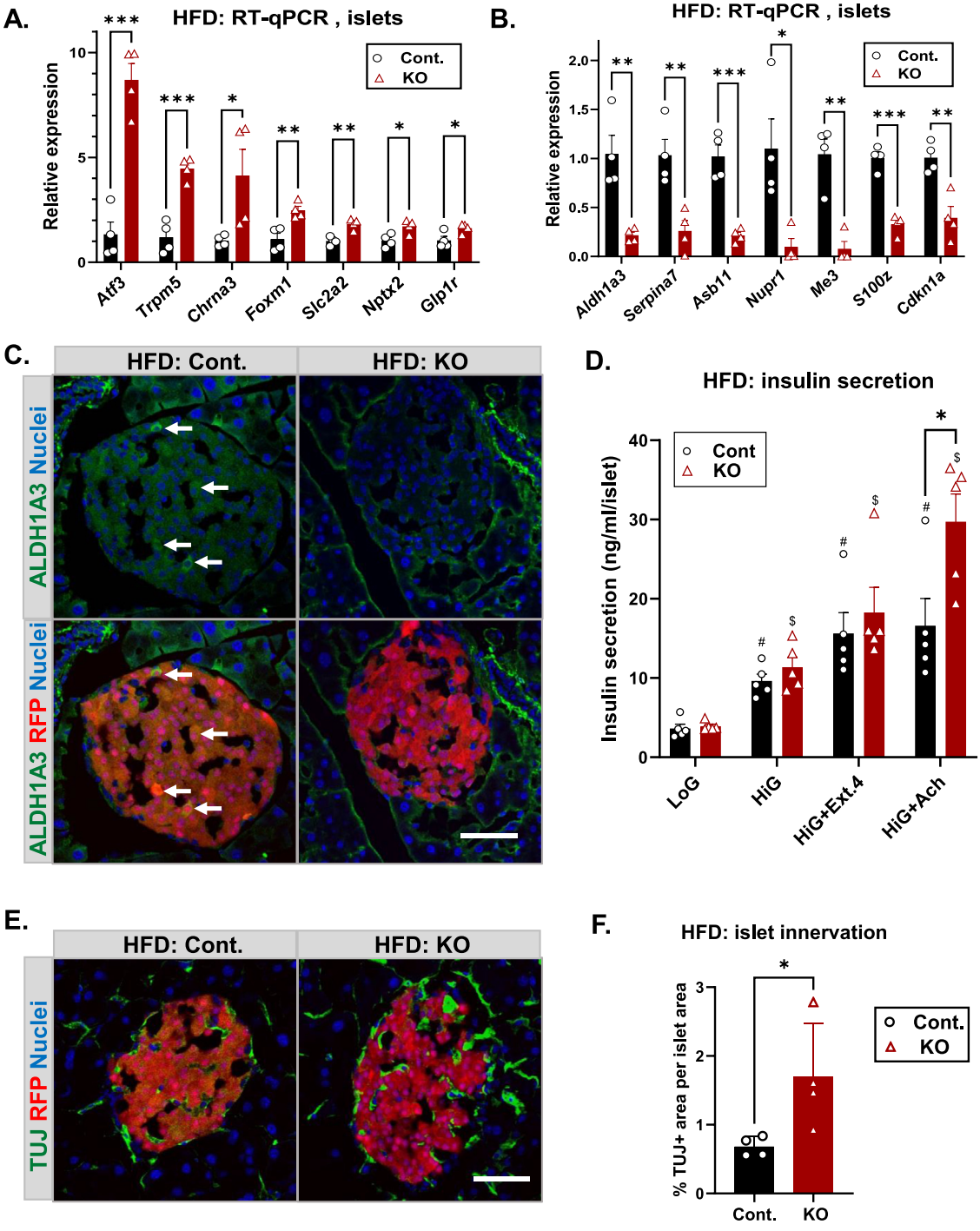

Figure 8: Decreased dedifferentiation and increased insulin secretion and islet innervation in *Ascl1*$^{\beta KO}$ islets on HFD. A) RT-qPCR analysis of islets from HFD-fed *Ascl1*$^{\beta KO}$ (KO) and control mice. Het HFD samples confirms upregulation of genes important for insulin secretion and downregulation of genes associated with β-cell dysfunction. N = 4. **B)** Representative images of immunofluorescent staining of pancreatic islet tissues from *Ascl1*$^{\beta KO}$ (KO) HFD and control (cont.) Het HFD mice for red fluorescent protein (RFP, red) that marks β-cells and β-cell dedifferentiation marker ALDH1A3 (green). Nuclei are stained with DAPI (blue). Arrows show ALDH1A3-positive β-cells. Control samples have higher levels of ALDH1A3 detected in β-cells. Scale bar: 50 μM. **C)** Glucose stimulated insulin secretion of *Ascl1*$^{\beta KO}$ (KO) HFD and control islets. Het HFD islets from *in vitro* static islet incubations. LoG (low glucose, 3.3 mM), HiG (high glucose 16.7 mM), Ext.4 (extendin-4, 1 μM), Ach (acetylcholine, 10 μM). *Ascl1*$^{\beta KO}$ samples show a stronger insulin secretion response to high glucose and acetylcholine than control samples. #p ≤ 0.01 Cont. samples compared to LoG control #p ≤ 0.01 KO samples compared to LoG KOs. **D)** Representative images of immunofluorescent staining for red fluorescent protein (RFP, red) that marks β-cells and neuronal marker TUJ (green) of *Ascl1*$^{\beta KO}$ and control Het samples. Nuclei are stained with DAPI (blue). **E)** Quantification of islet innervation (TUJ-positive areas per total islet areas). N = 4. All mice are males, 17 weeks old. Error bars: ±SEM. ***p ≤ 0.001, **p ≤ 0.01, *p ≤ 0.05. p-values were determined by t-test. (For interpretation of the references to color in this figure legend, the reader is referred to the Web version of this article.)

transcription being regulated by depolarization induced entry of Ca^{2+} through VDCCs on the plasma membrane and signaling to the nucleus via CREB. Similarly, in neurons, increases in Ca^{2+} oscillations [53] and CREB activation [54] were shown to increase *Ascl1* expression. While Ca^{2+}-dependent transcriptional regulation by CREB is critical for the response of excitable cells to environmental cues, prolonged CREB activation is unhealthy and has adverse effects [55,56]. We show that *Ascl1* expression is dependent on Ca^{2+}-signaling and that it is activated in metabolically stressed β-cells. However, other pathways are likely to also contribute to *Ascl1* regulation in response to a HFD. While this study was done in mice, our findings likely extend to humans since β-cells from people with T2D with low *INS* gene expression have higher *ASCL1* expression. Furthermore, in human islets the chromatin surrounding *ASCL1* is open [57], suggesting that the gene is poised to respond to an increase in $[Ca^{2+}]_i$.

4.2. Role of *Ascl1* in pancreatic β-cells and metabolic stress response

Analysis of *Ascl1*$^{\beta KO}$ mice fed a normal diet revealed no differences in glucose handling, insulin secretion, β-cell area, or hormone cell composition in adult islets. While transcriptional analysis revealed changes in the islet transcriptome of *Ascl1*$^{\beta KO}$ compared to wild type mice, these data further confirm that *Ascl1* is not required for normal β-cell development and function. Although changes occur in the transcriptome of islets from *Ascl1*$^{\beta KO}$ mice on ND that include many secretory and ER genes, they do not cause any readily detectable functional impairments. We also did not observe any changes in glucose homeostasis or islet structure when *Ascl1* was eliminated from β-cells of *Abcc8* KO mice. This is surprising since *Ascl1* is highly expressed in *Abcc8* KO mice, and was predicted to regulate dedifferentiation genes up-regulated in β-cell by excitotoxicity [19]. The lack of any improvement in islet function in the double KO mice (*Ascl1*$^{\beta KO}$; *Abcc8* KO) indicates that ASCL1 does not contribute to the impairments in β-cell function brought on by the lack of functional K_{ATP} channels. Instead, genes involved in ER stress and the unfolded protein response, including the pro-apoptotic gene *Ddit3* (*Chop*) [58], are upregulated while hormone secretion genes are downregulated in the absence of *Ascl1*. Since ER stress due to increased insulin secretory demand contributes to β-cell dysfunction [47], ASCL1-driven dedifferentiation may serve to protect β-cells from the adverse effects of temporary insulin hypersecretion brought on by chronic membrane depolarization [59]. In any case, the disruption of *Ascl1* in mice lacking *Abcc8* does not result in further impairment of β-cell function. Thus, other yet to be identified transcription factors may be principally responsible for the many gene expression changes observed in *Abcc8* KO β-cells.

The most pronounced, and beneficial, effect of eliminating *Ascl1* in β-cells occurred in the setting of HFD-driven metabolic stress where we observed a decrease in blood glucose, increased glucose tolerance and increased β-cell proliferation in comparison to controls. Furthermore, we observed broader changes in transcriptome with changes in many genes that are affected by HFD being reversed in *Ascl1*$^{\beta KO}$ islets and included decreases in the dedifferentiation genes *Aldh1a3* and *S100z* [41,60], and the immature and aging β-cell marker *Bambi* [61]. We also observed an increase in expression of genes associated with insulin secretion (*Slc2a2*, *Glp1r*, *Mafa*) and β-cell proliferation (*Foxm1*) further indicating that the transcriptional regulation of these and other genes by ASCL1 contributes to β-cell failure during metabolic stress, and that the deletion of *Ascl1* protects β-cells from negative effects of HFD.

Notably, some unexpected genes were increased in *Ascl1*$^{\beta KO}$ islets from animals on a HFD. These included several neuronal peptides including gastrin-releasing peptide (*Grp*) and vasoactive intestinal peptide (*Vip*). While these peptides can be produced by islet cells, they are mostly secreted by parasympathetic neurons that innervate islets and stimulate insulin secretion [62,63]. We also detected an increase in *Slc18a3*, the acetylcholine transporter (or VAchT) and *Nos1* (n-NOS). Because both are markers of parasympathetic nerves, we studied the A*scl1*$^{\beta KO}$ mice further and found an increase in neural fibers in *Ascl1*$^{\beta KO}$ islets and improved secretion of isolated islets in response to acetylcholine. In islets, acetylcholine released by parasympathetic neurons and α-cells potentiate insulin secretion via muscarinic 3 cholinergic receptors [64]. While our RNA-seq results did not show any changes in muscarinic receptor expression, there was an increase in expression of the nicotinic cholinergic receptors (nAChRs) *Chrna3*, *Chrnb4* and *Chrna7*. These changes could either be the result of increased innervation or could be caused by changes in *Ascl1* KO β-cells since nicotinic receptors have been shown to be expressed in β-cells [65–67]. In either case, signaling through nAChRs has previously been shown to increase insulin secretion in β-cells [65,68], to improve β-cell function, and to protect β-cells from apoptosis [69,70] and ER stress [71]. ASCL1 has also been shown to regulate *CHRNA3/B4* in lung cancer [72]. Thus, it is possible that an increase in nAChR expression in the absence of *Ascl1* could also cause the increase in acetylcholine response and improvement in β-cell function that we observed. Parasympathetic signaling was also shown to contribute to FOXM1-driven β-cell proliferation in obesity [73]. Together, these findings suggest that the improvements in β-cell function and increased proliferation that occur in *Ascl1*$^{\beta KO}$ mice fed a HFD may be at least partially due to an increase in islet innervation and increased acetylcholine signaling.

It is not clear how a deletion of *Ascl1* in β-cells leads to an increase in islet innervation, however, β-cells are known to produce factors that promote the ingrowth of nerve fibers [74]. In *Ascl1*$^{\beta KO}$ islets the observed increases in expression of neuropeptides and genes encoding neural guidance adhesion molecules (*Nptx2*, *Pcdh7*, *Slit2*) could all contribute to increased innervation. Paracrine signaling between neural and endocrine cells helps to adapt islet function to body insulin demand and the term "neuro-islet plasticity" has been proposed to describe an increase in islet innervation in order to maintain insulin secretion under metabolic stress [75]. The increases we observe in both islet innervation and function in metabolically stressed islets in the absence of *Ascl1* suggest that transcriptional regulation by ASCL1 represses this process.

4.3. Transcriptional regulation by ASCL1 in β-cells is context-dependent

The marked variations in transcriptional responses in *Ascl1*$^{\beta KO}$ in different conditions suggest a complex and context-dependent nature of transcriptional regulation by ASCL1 in β-cells. ASCL1 is known to form heterodimers with other bHLH neuronal transcription factors [10] and to interact with various transcriptional co-regulators [76] to exert its effects. Thus, both the binding and actions of ASCL1 may be highly dependent on the combination of transcription factors expressed in β-cells at a given condition. Indeed, it has been suggested that combinatorial binding by various bHLH in heterodimers forms a "bHLH code" where different combinations of bHLH factors bind slightly different E-box sequences to differentially drive the expression of target genes [77]. For example, in neurons, ASCL1 and NEUROG2 alone or in combination together bind to different sequences [78]. In β-cells, metabolic-stress induced ASCL1 and co-regulators may stimulate or block the binding of other bHLH proteins to their cognate elements, thereby affecting gene expression in a highly complex manner. For instance, prediction analysis of TFs that drive genes upregulated on HFD in the absence of *Ascl1* predicts NEUROD1, a TF important for mature β-cell function [63], as one of

the top regulators. Therefore, it is possible that the induction of ASCL1 by metabolic stress may displace NEUROD1 from target sites, down-regulating the expression of key target genes and impeding β-cell function. In addition, since ASCL1 is a pioneer transcription factor [16] that can bind to a closed chromatin by itself or in combination with other transcriptional regulators, the induction of ASCL1 may affect the epigenetic state of β-cells, impairing their ability to maintain their identity. Further characterization of ASCL1 binding sites and analysis of interacting partners in β-cells during metabolic stress is needed to precisely identify target genes and to better understand how a Ca^{2+}-dependent gene network contributes to the metabolic-stress responses of β-cells.

5. CONCLUSIONS

Ascl1 expression is induced by metabolic stress and increases in Ca^{2+} signaling to the nucleus and contributes to β-cell failure by activating dedifferentiation program and suppressing genes important for mature β-cell function and parasympathetic innervation. These data provide new insights into the mechanisms by which the metabolic stress associated with overnutrition may lead to a loss in β-cell function and the development of T2D.

FUNDING

This study was supported by institutional and philanthropic funds from Vanderbilt University. The Vanderbilt Islet and Pancreas Analysis Core is supported by NIH grant DK020593, the Hormone Assay and Analytical Services Core is supported by NIH grants DK059637 and DK020593, Vanderbilt Cell Imaging Shared Resource (CISR) Core is supported by NIH grants CA68485, DK20593, DK58404, DK59637 and EY08126.

AUTHOR CONTRIBUTIONS

ABO: Conceptualization, Investigation, Data Curation, Formal Analysis, Methodology, Validation, Visualization, Supervision, Writing — Original Draft Preparation, Writing — Review & Editing.
FYZ: Investigation, Data Curation, Methodology, Validation.
JJC: Investigation, Data Curation, Methodology, Validation.
LTT: Investigation, Data Curation.
MAC: Data Curation, Methodology, Software, Visualization.
SS: Data Curation, Methodology, Software, Visualization.
JPC: Data Curation, Methodology, Software, Visualization.
MAM: Conceptualization, Project Administration, Funding Acquisition, Supervision, Resources, Writing — Review & Editing.

DATA STATEMENT

RNA-Seq data are available in ArrayExpress (https://www.ebi.ac.uk/arrayexpress) under accession number E-MTAB-13355.

DECLARATION OF COMPETING INTEREST

The authors declare that they have no known competing financial interests or personal relationships that could have appeared to influence the work reported in this paper.

DATA AVAILABILITY

No data was used for the research described in the article.

ACKNOWLEDGMENTS

We thank Lily H. Kim for mouse genotyping and Marcella Brissova for providing antibodies. RNA-Seq data analysis was performed by Creative Data Solutions (RRID:SCR_022366) using the Advanced Computing Center for Research and Education (ACCRE) at Vanderbilt University.

APPENDIX A. SUPPLEMENTARY DATA

Supplementary data to this article can be found online at https://doi.org/10.1016/j.molmet.2023.101811.

REFERENCES

[1] Bensellam M, Laybutt DR, Jonas JC. The molecular mechanisms of pancreatic beta-cell glucotoxicity: recent findings and future research directions. Mol Cell Endocrinol 2012;364(1—2):1—27.
[2] Chang-Chen KJ, Mullur R, Bernal-Mizrachi E. Beta-cell failure as a complication of diabetes. Rev Endocr Metab Disord 2008;9(4):329—43.
[3] Muoio DM, Newgard CB. Mechanisms of disease: molecular and metabolic mechanisms of insulin resistance and beta-cell failure in type 2 diabetes. Nat Rev Mol Cell Biol 2008;9(3):193—205.
[4] Chen C, Chmelova H, Cohrs CM, Chouinard JA, Jahn SR, Stertmann J, et al. Alterations in beta-cell calcium dynamics and efficacy outweigh islet mass adaptation in compensation of insulin resistance and prediabetes onset. Diabetes 2016;65(9):2676—85.
[5] Talchai C, Xuan S, Lin HV, Sussel L, Accili D. Pancreatic beta cell dedifferentiation as a mechanism of diabetic beta cell failure. Cell 2012;150(6):1223—34.
[6] Cinti F, Bouchi R, Kim-Muller JY, Ohmura Y, Sandoval PR, Masini M, et al. Evidence of beta-cell dedifferentiation in human type 2 diabetes. J Clin Endocrinol Metab 2016;101(3):1044—54.
[7] Bensellam M, Jonas JC, Laybutt DR. Mechanisms of beta-cell dedifferentiation in diabetes: recent findings and future research directions. J Endocrinol 2018;236(2):R109—43.
[8] Efrat S. Beta-cell dedifferentiation in type 2 diabetes: concise review. Stem Cells 2019;37(10):1267—72.
[9] Vasconcelos FF, Castro DS. Transcriptional control of vertebrate neurogenesis by the proneural factor Ascl1. Front Cell Neurosci 2014;8:412.
[10] Bertrand N, Castro DS, Guillemot F. Proneural genes and the specification of neural cell types. Nat Rev Neurosci 2002;3(7):517—30.
[11] Imayoshi I, Isomura A, Harima Y, Kawaguchi K, Kori H, Miyachi H, et al. Oscillatory control of factors determining multipotency and fate in mouse neural progenitors. Science 2013;342(6163):1203—8.
[12] Chanda S, Ang CE, Davila J, Pak C, Mall M, Lee QY, et al. Generation of induced neuronal cells by the single reprogramming factor ASCL1. Stem Cell Rep 2014;3(2):282—96.
[13] Ball DW. Achaete-scute homolog-1 and Notch in lung neuroendocrine development and cancer. Cancer Lett 2004;204(2):159—69.
[14] Kokubu H, Ohtsuka T, Kageyama R. Mash1 is required for neuroendocrine cell development in the glandular stomach. Genes Cells 2008;13(1):41—51.
[15] Huber K, Bruhl B, Guillemot F, Olson EN, Ernsberger U, Unsicker K. Development of chromaffin cells depends on MASH1 function. Development 2002;129(20):4729—38.
[16] Raposo A, Vasconcelos FF, Drechsel D, Marie C, Johnston C, Dolle D, et al. Ascl1 coordinately regulates gene expression and the chromatin landscape during neurogenesis. Cell Rep 2015;10(9):1544—56.
[17] Park NI, Guilhamon P, Desai K, McAdam RF, Langille E, O'Connor M, et al. ASCL1 reorganizes chromatin to direct neuronal fate and suppress tumorigenicity of glioblastoma stem cells. Cell Stem Cell 2017;21(2):209—224 e207.

[18] Osipovich AB, Stancill JS, Cartailler JP, Dudek KD, Magnuson MA. Excitotoxicity and overnutrition additively impair metabolic function and identity of pancreatic beta-cells. Diabetes 2020;69(7):1476–91.
[19] Stancill JS, Cartailler JP, Clayton HW, O'Connor JT, Dickerson MT, Dadi PK, et al. Chronic beta-cell depolarization impairs beta-cell identity by disrupting a network of Ca2+-regulated genes. Diabetes 2017;66(8):2175–87.
[20] Shiota C, Larsson O, Shelton KD, Shiota M, Efanov AM, Hoy M, et al. Sulfonylurea receptor type 1 knock-out mice have intact feeding-stimulated insulin secretion despite marked impairment in their response to glucose. J Biol Chem 2002;277(40):37176–83.
[21] Nasteska D, Fine NHF, Ashford FB, Cuozzo F, Viloria K, Smith G, et al. PDX1(LOW) MAFA(LOW) beta-cells contribute to islet function and insulin release. Nat Commun 2021;12(1):674.
[22] Flasse LC, Pirson JL, Stern DG, Von Berg V, Manfroid I, Peers B, et al. Ascl1b and Neurod1, instead of Neurog3, control pancreatic endocrine cell fate in zebrafish. BMC Biol 2013;11:78.
[23] Schwitzgebel VM, Scheel DW, Conners JR, Kalamaras J, Lee JE, Anderson DJ, et al. Expression of neurogenin3 reveals an islet cell precursor population in the pancreas. Development 2000;127(16):3533–42.
[24] Ackermann AM, Wang Z, Schug J, Naji A, Kaestner KH. Integration of ATAC-seq and RNA-seq identifies human alpha cell and beta cell signature genes. Mol Metab 2016;5(3):233–44.
[25] Pasquali L, Gaulton KJ, Rodriguez-Segui SA, Mularoni L, Miguel-Escalada I, Akerman I, et al. Pancreatic islet enhancer clusters enriched in type 2 diabetes risk-associated variants. Nat Genet 2014;46(2):136–43.
[26] Whyte WA, Orlando DA, Hnisz D, Abraham BJ, Lin CY, Kagey MH, et al. Master transcription factors and mediator establish super-enhancers at key cell identity genes. Cell 2013;153(2):307–19.
[27] Pacary E, Heng J, Azzarelli R, Riou P, Castro D, Lebel-Potter M, et al. Proneural transcription factors regulate different steps of cortical neuron migration through Rnd-mediated inhibition of RhoA signaling. Neuron 2011;69(6):1069–84.
[28] Thorens B, Tarussio D, Maestro MA, Rovira M, Heikkila E, Ferrer J. Ins1(Cre) knock-in mice for beta cell-specific gene recombination. Diabetologia 2015;58(3):558–65.
[29] Madisen L, Zwingman TA, Sunkin SM, Oh SW, Zariwala HA, Gu H, et al. A robust and high-throughput Cre reporting and characterization system for the whole mouse brain. Nat Neurosci 2010;13(1):133–40.
[30] Dobin A, Davis CA, Schlesinger F, Drenkow J, Zaleski C, Jha S, et al. STAR: ultrafast universal RNA-seq aligner. Bioinformatics 2013;29(1):15–21.
[31] Love MI, Huber W, Anders S. Moderated estimation of fold change and dispersion for RNA-seq data with DESeq2. Genome Biol 2014;15(12):550.
[32] Zhou Y, Zhou B, Pache L, Chang M, Khodabakhshi AH, Tanaseichuk O, et al. Metascape provides a biologist-oriented resource for the analysis of systems-level datasets. Nat Commun 2019;10(1):1523.
[33] Qin Q, Fan J, Zheng R, Wan C, Mei S, Wu Q, et al. Lisa: inferring transcriptional regulators through integrative modeling of public chromatin accessibility and ChIP-seq data. Genome Biol 2020;21(1):32.
[34] Patil AR, Schug J, Naji A, Kaestner KH, Faryabi RB, Vahedi G. Single-cell expression profiling of islets generated by the human pancreas analysis program. Nat Metab 2023;5(5):713–5.
[35] Wolf FA, Angerer P, Theis FJ. SCANPY: large-scale single-cell gene expression data analysis. Genome Biol 2018;19(1):15.
[36] Osipovich AB, Gangula R, Vianna PG, Magnuson MA. Setd5 is essential for mammalian development and the co-transcriptional regulation of histone acetylation. Development 2016;143(24):4595–607.
[37] Schneider CA, Rasband WS, Eliceiri KW. NIH Image to ImageJ: 25 years of image analysis. Nat Methods 2012;9(7):671–5.
[38] Osipovich AB, Dudek KD, Greenfest-Allen E, Cartailler JP, Manduchi E, Potter Case L, et al. A developmental lineage-based gene co-expression network for mouse pancreatic beta-cells reveals a role for Zfp800 in pancreas development. Development 2021;148(6).
[39] Bengtson CP, Bading H. Nuclear calcium signaling. Adv Exp Med Biol 2012;970:377–405.
[40] Kim-Muller JY, Fan J, Kim YJ, Lee SA, Ishida E, Blaner WS, et al. Aldehyde dehydrogenase 1a3 defines a subset of failing pancreatic beta cells in diabetic mice. Nat Commun 2016;7:12631.
[41] Jonas W, Kluth O, Helms A, Voss S, Jahnert M, Gottmann P, et al. Identification of novel genes involved in hyperglycemia in mice. Int J Mol Sci 2022;23(6).
[42] Henquin JC. Triggering and amplifying pathways of regulation of insulin secretion by glucose. Diabetes 2000;49(11):1751–60.
[43] Gilon P, Chae HY, Rutter GA, Ravier MA. Calcium signaling in pancreatic beta-cells in health and in Type 2 diabetes. Cell Calcium 2014;56(5):340–61.
[44] Sabatini PV, Speckmann T, Lynn FC. Friend and foe: beta-cell Ca(2+) signaling and the development of diabetes. Mol Metab 2019;21:1–12.
[45] Do OH, Low JT, Gaisano HY, Thorn P. The secretory deficit in islets from db/db mice is mainly due to a loss of responding beta cells. Diabetologia 2014;57(7):1400–9.
[46] Bano D, Nicotera P. Ca^{2+} signals and neuronal death in brain ischemia. Stroke 2007;38(2 Suppl):674–6.
[47] Dong XX, Wang Y, Qin ZH. Molecular mechanisms of excitotoxicity and their relevance to pathogenesis of neurodegenerative diseases. Acta Pharmacol Sin 2009;30(4):379–87.
[48] Bompotis GC, Deftereos S, Angelidis C, Choidis E, Panagopoulou V, Kaoukis A, et al. Altered calcium handling in reperfusion injury. Med Chem 2016;12(2):114–30.
[49] Verma M, Wills Z, Chu CT. Excitatory dendritic mitochondrial calcium toxicity: implications for Parkinson's and other neurodegenerative diseases. Front Neurosci 2018;12:523.
[50] Arntfield ME, van der Kooy D. beta-Cell evolution: how the pancreas borrowed from the brain: the shared toolbox of genes expressed by neural and pancreatic endocrine cells may reflect their evolutionary relationship. Bioessays 2011;33(8):582–7.
[51] Wang S, Yan J, Anderson DA, Xu Y, Kanal MC, Cao Z, et al. Neurog3 gene dosage regulates allocation of endocrine and exocrine cell fates in the developing mouse pancreas. Dev Biol 2010;339(1):26–37.
[52] Osipovich AB, Long Q, Manduchi E, Gangula R, Hipkens SB, Schneider J, et al. Insm1 promotes endocrine cell differentiation by modulating the expression of a network of genes that includes Neurog3 and Ripply3. Development 2014;141(15):2939–49.
[53] Glaser T, Shimojo H, Ribeiro DE, Martins PPL, Beco RP, Kosinski M, et al. ATP and spontaneous calcium oscillations control neural stem cell fate determination in Huntington's disease: a novel approach for cell clock research. Mol Psychiatry 2021;26(6):2633–50.
[54] Gascon S, Ortega F, Gotz M. Transient CREB-mediated transcription is key in direct neuronal reprogramming. Neurogenesis 2017;4(1):e1285383.
[55] Dewenter M, von der Lieth A, Katus HA, Backs J. Calcium signaling and transcriptional regulation in cardiomyocytes. Circ Res 2017;121(8):1000–20.
[56] Hagenston AM, Bading H, Bas-Orth C. Functional consequences of calcium-dependent synapse-to-nucleus communication: focus on transcription-dependent metabolic plasticity. Cold Spring Harb Perspect Biol 2020;12(4).
[57] Mularoni L, Ramos-Rodriguez M, Pasquali L. The pancreatic islet regulome browser. Front Genet 2017;8:13.

[58] Oyadomari S, Koizumi A, Takeda K, Gotoh T, Akira S, Araki E, et al. Targeted disruption of the Chop gene delays endoplasmic reticulum stress-mediated diabetes. J Clin Investig 2002;109(4):525–32.
[59] Seghers V, Nakazaki M, DeMayo F, Aguilar-Bryan L, Bryan J. Sur1 knockout mice. A model for K(ATP) channel-independent regulation of insulin secretion. J Biol Chem 2000;275(13):9270–7.
[60] Son J, Du W, Esposito M, Shariati K, Ding H, Kang Y, et al. Genetic and pharmacologic inhibition of ALDH1A3 as a treatment of beta-cell failure. Nat Commun 2023;14(1):558.
[61] Aguayo-Mazzucato C, van Haaren M, Mruk M, Lee Jr TB, Crawford C, Hollister-Lock J, et al. Beta cell aging markers have heterogeneous distribution and are induced by insulin resistance. Cell Metab 2017;25(4):898–910 e895.
[62] Karlsson S, Sundler F, Ahren B. Insulin secretion by gastrin-releasing peptide in mice: ganglionic versus direct islet effect. Am J Physiol 1998;274(1):E124–9.
[63] Winzell MS, Ahren B. Role of VIP and PACAP in islet function. Peptides 2007;28(9):1805–13.
[64] Noguchi GM, Huising MO. Integrating the inputs that shape pancreatic islet hormone release. Nat Metab 2019;1(12):1189–201.
[65] Yoshikawa H, Hellstrom-Lindahl E, Grill V. Evidence for functional nicotinic receptors on pancreatic beta cells. Metabolism 2005;54(2):247–54.
[66] Somm E, Guerardel A, Maouche K, Toulotte A, Veyrat-Durebex C, Rohner-Jeanrenaud F, et al. Concomitant alpha7 and beta2 nicotinic AChR subunit deficiency leads to impaired energy homeostasis and increased physical activity in mice. Mol Genet Metab 2014;112(1):64–72.
[67] Delbro DS. Expression of the non-neuronal cholinergic system in rat beta-cells. Auton Neurosci 2012;167(1–2):75–7.
[68] Ganic E, Singh T, Luan C, Fadista J, Johansson JK, Cyphert HA, et al. MafA-controlled nicotinic receptor expression is essential for insulin secretion and is impaired in patients with type 2 diabetes. Cell Rep 2016;14(8):1991–2002.
[69] Klee P, Bosco D, Guerardel A, Somm E, Toulotte A, Maechler P, et al. Activation of nicotinic acetylcholine receptors decreases apoptosis in human and female murine pancreatic islets. Endocrinology 2016;157(10):3800–8.
[70] Gupta D, Lacayo AA, Greene SM, Leahy JL, Jetton TL. beta-Cell mass restoration by alpha7 nicotinic acetylcholine receptor activation. J Biol Chem 2018;293(52):20295–306.
[71] Ishibashi T, Morita S, Kishimoto S, Uraki S, Takeshima K, Furukawa Y, et al. Nicotinic acetylcholine receptor signaling regulates inositol-requiring enzyme 1alpha activation to protect beta-cells against terminal unfolded protein response under irremediable endoplasmic reticulum stress. J Diabetes Investig 2020;11(4):801–13.
[72] Improgo MR, Schlichting NA, Cortes RY, Zhao-Shea R, Tapper AR, Gardner PD. ASCL1 regulates the expression of the CHRNA5/A3/B4 lung cancer susceptibility locus. Mol Cancer Res 2010;8(2):194–203.
[73] Yamamoto J, Imai J, Izumi T, Takahashi H, Kawana Y, Takahashi K, et al. Neuronal signals regulate obesity induced beta-cell proliferation by FoxM1 dependent mechanism. Nat Commun 2017;8(1):1930.
[74] Myrsen U, Keymeulen B, Pipeleers DG, Sundler F. Beta cells are important for islet innervation: evidence from purified rat islet-cell grafts. Diabetologia 1996;39(1):54–9.
[75] Ahrén B, Wierup N, Sundler F. Neuropeptides and the regulation of islet function. Diabetes 2006;55(Supplement_2):S98–107.
[76] Tarczewska A, Greb-Markiewicz B. The significance of the intrinsically disordered regions for the functions of the bHLH transcription factors. Int J Mol Sci 2019;20(21).
[77] Conway SJ, Firulli B, Firulli AB. A bHLH code for cardiac morphogenesis. Pediatr Cardiol 2010;31(3):318–24.
[78] Aydin B, Kakumanu A, Rossillo M, Moreno-Estelles M, Garipler G, Ringstad N, et al. Proneural factors Ascl1 and Neurog2 contribute to neuronal subtype identities by establishing distinct chromatin landscapes. Nat Neurosci 2019;22(6):897–908.

